

Novel Properties of Cooperative Dinuclear Zinc(II) Ions: The Selective Recognition of Phosphomonoesters and Their P–O Ester Bond Cleavage by a New Dinuclear Zinc(II) Cryptate

Tohru Koike,[†] Masaki Inoue,[†] Eiichi Kimura,^{*,†} and Motoo Shiro[‡]

Contribution from the Department of Medicinal Chemistry, School of Medicine, Hiroshima University, Kasumi 1-2-3, Minami-ku, Hiroshima, 734, Japan, and Rigaku Corporation X-ray Research Laboratory, Matsubaracho 3-9-12, Akishima, Tokyo, 196, Japan

Received October 10, 1995[⊗]

Abstract: A propanol-bridged octaazacryptand (26-hydroxy-1,4,7,10,13,16,19,22-octaazabicyclo[11.11.3]heptacosane, HL) has been synthesized from diethylenetriamine and [2-oxo-6-(aminomethyl)morpholy]-*N,N',N'*-triacetic acid triethyl ester by refluxing in MeOH followed by $\text{BH}_3 \cdot \text{THF}$ reduction. This octaazacryptand forms a novel dinuclear zinc(II) cryptate (Zn_2L) (L = alkoxide form of HL) in aqueous solution. The X-ray crystal structure of the cryptate showed each zinc(II) ion in a distorted trigonal-bipyramidal environment involving two NH's and an alkoxide O^- anion as equatorial donors, with tertiary amine and an NH stand in apical positions. Crystals of the triperchlorate salt of Zn_2L ($\text{C}_{19}\text{H}_{43}\text{N}_8\text{O}_{15}\text{Cl}_3\text{Zn}_2$) are monoclinic, space group $P2_1/n$ (No. 14) with $a = 15.037(5)$ Å, $b = 13.862(5)$ Å, $c = 15.780(4)$ Å, $\beta = 90.29(2)^\circ$, $Z = 4$, and $R = 0.109$. Although the two zinc(II) ions (separated with a distance of 3.42 Å) in the cryptate appeared to be coordinately saturated and hence were assumed unreactive, they work together to selectively interact with a phosphomonoester, 4-nitrophenyl phosphate dianion (NPP^{2-}), and promote the cleavage of its P–O ester bond by nucleophilic attack of one of the apically coordinated NH's at pH 4.9–9.5 in aqueous solution. The reaction product was isolated as a phosphoramidate derivative ($\text{Zn}_2\text{L}-\text{PO}_3\text{H}$) from aqueous solution at pH 3 and characterized by X-ray crystal analysis. Crystals of $\text{Zn}_2\text{L}-\text{PO}_3\text{H} \cdot 2\text{H}_2\text{O} \cdot (\text{ClO}_4)_3$ ($\text{C}_{19}\text{H}_{48}\text{N}_8\text{O}_{18}\text{Cl}_3\text{Zn}_2$) are monoclinic, space group Cc (No. 9) with $a = 19.573(3)$ Å, $b = 12.454(4)$ Å, $c = 15.066(3)$ Å, $\beta = 103.94(1)^\circ$, $Z = 4$, and $R = 0.036$. The structure of $\text{Zn}_2\text{L}-\text{PO}_3\text{H}$ featured the two phosphoryl oxygens bound to each zinc(II) ion in place of the original two apical NH's. The kinetics were followed for liberation of 4-nitrophenol (the maximum second-order rate constant $k_{\text{NPP}} = (1.52 \pm 0.05) \times 10^{-3} \text{ M}^{-1} \text{ s}^{-1}$ at pH 5.9 and 35 °C). The rate vs pH profile with 5 mM Zn_2L and 10 mM 4-nitrophenyl phosphate showed a bell-shaped curve with $\text{p}K_1$ of 5.2 and $\text{p}K_2$ of 6.3, which were assigned to the protonation constants for $\text{NPP}^{2-} + \text{H} \rightleftharpoons \text{HNPP}^-$ and NH (a freed apical donor in the associated reaction intermediate) $+ \text{H}^+ \rightleftharpoons \text{HNH}^+$, respectively. The most remarkable character of the present new zinc(II) cryptate was that it reacted only with phosphoester polyanions such as NPP^{2-} and ATP^{4-} , but not with bis(4-nitrophenyl) phosphodiester monoanion, tris(4-nitrophenyl) phosphotriester, or 4-nitrophenyl acetate. The present results may well be relevant to the significance of dinuclear metal centers in metallophosphatases such as alkaline monophosphatase.

Introduction

Alkaline phosphatase (AP) is a Zn^{II} -containing phosphomonoesterase that selectively hydrolyzes phosphomonoester dianion by using the two cooperative zinc(II) ions at the active center.¹ There have been numerous reports of phosphoesterase model systems using metal complexes, but most of these models were aimed at achieving faster hydrolysis of phosphate,^{2,3} and as yet, few systematical models concentrate on the selective reaction toward the substrate phosphomonoester dianion.

In the course of an attempt to synthesize a new ligand **4** for a phosphomonoesterase model (a bis(macrocylic tetraamine) linked by a 2-hydroxypropyl group from a carboxyester (**1**) and diethylenetriamine (**2**)), we incidentally isolated an isomeric (of **3**) tetraoxocryptand **6** as a main product, which was an intermediate for a new octaazacryptand **7** (see Scheme 1). The purpose of the synthesis of **4** was to prepare a dinuclear zinc(II) complex **5**, which may lead to a novel alkaline phosphatase model. With all the previous phosphatase models composite of mononuclear metal complexes studied by us^{4,5} and other groups,^{2,3} hydrolyses of carboxyesters, phosphotriesters, phosphodiesters, and phosphomonoesters were successful. However,

R. J. Am. Chem. Soc. **1986**, *108*, 2388–2394. (j) Chin, J.; Banaszczyk, M.; Jubian, V.; Zou, X. J. Am. Chem. Soc. **1989**, *111*, 186–190. (k) Hendry, P.; Sargeson, A. M. J. Am. Chem. Soc. **1989**, *111*, 2521–2527. (l) Morrow, J. R.; Trogler, W. C. Inorg. Chem. **1988**, *27*, 3387–3394.

(3) Dinuclear system: (a) Vance, D. H.; Czarnik, A. W. J. Am. Chem. Soc. **1993**, *115*, 12165–12166. (b) Hikichi, S.; Tanaka, M.; Morooka, Y.; Kitajima, N. J. Chem. Soc., Chem. Commun. **1992**, 814–815. (c) Chung, Y.; Akkaya, E. U.; Venkatachalam, T. K.; Czarnik, A. W. Tetrahedron Lett. **1990**, *31*, 5413–5416. (d) Takasaki, B. K.; Chin, J. J. Am. Chem. Soc. **1995**, *117*, 8582–8585. (e) Connolly, J. A.; Banaszczyk, M.; Hynes, R. C.; Chin, J. Inorg. Chem. **1994**, *33*, 665–669. (f) Chapman, W. H., Jr.; Breslow, R. J. Am. Chem. Soc. **1995**, *117*, 5462–5469. (g) Clewley, R. G.; Slesbocka-Tilk, H.; Brown, R. S. Inorg. Chim. Acta **1989**, *157*, 233–238.

(4) Koike, T.; Kimura, E. J. Am. Chem. Soc. **1991**, *113*, 8935–8941.

[†] Hiroshima University.

[‡] Rigaku Corp.

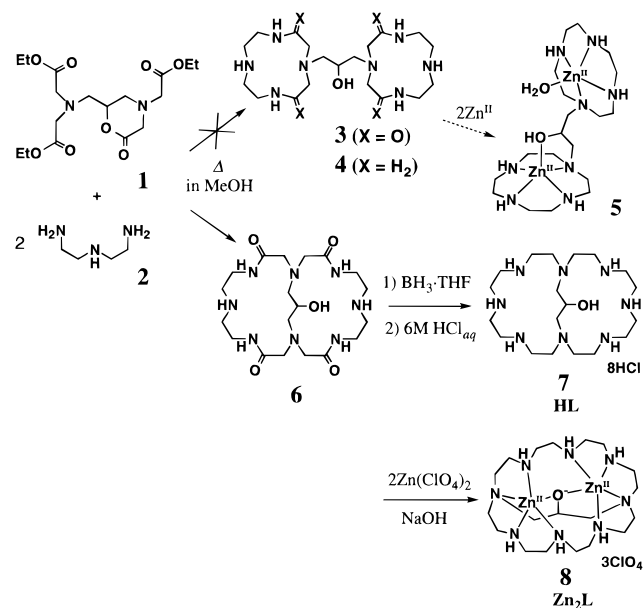
* e-mail: ekimura@ue.ipc.hiroshima-u.ac.jp.

⊗ Abstract published in *Advance ACS Abstracts*, March 15, 1996.

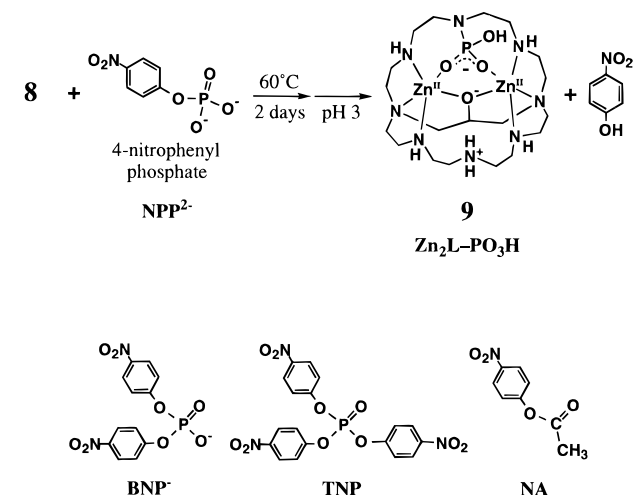
(1) (a) Kim, E. E.; Wyckoff, H. W. J. Mol. Biol. **1991**, *218*, 449–464. (b) Coleman, J. E. Annu. Rev. Biophys. Biomol. Struct. **1992**, *21*, 441–483.

(2) Mononuclear system: (a) Jones, D. R.; Lindoy, L. F.; Sargeson, A. M. J. Am. Chem. Soc. **1983**, *105*, 7327–7336. (b) Tsubouchi, A.; Bruce, T. C. J. Am. Chem. Soc. **1994**, *116*, 11614–11615. (c) Sigman, D. S.; Wahl, G. M.; Creighton, D. J. Biochemistry **1972**, *11*, 2236–2242. (d) Tafesse, F.; Massoud, S. S.; Milburn, R. M. Inorg. Chem. **1993**, *32*, 1864–1865. (e) Norman, P. R.; Cornelius, R. D. J. Am. Chem. Soc. **1982**, *104*, 2356–2361. (f) De Rosch, M. A.; Trogler, W. C. Inorg. Chem. **1990**, *29*, 2409–2416. (g) Hay, R. W.; Govan, N. J. Chem. Soc., Chem. Commun. **1990**, 714–715. (h) Ruf, M.; Weis, K.; Vahrenkamp, H. J. Chem. Soc., Chem. Commun. **1994**, 135–136. (i) Gellman, S. H.; Petter, R.; Breslow,

Scheme 1



Scheme 2



they did not focus on the selective hydrolysis of the substrate phosphomonoesters. In our recent work,⁵ we discovered that the zinc(II) complexes with macrocyclic polyamines bearing an alcohol pendant (*N*-hydroxyethyl group) promote efficiently the hydrolysis of acetate and phosphodiester. Therefore, we attempted to combine dinuclear zinc(II) and an alcohol pendant in **5** to build a phosphomonoesterase model.

However, a new dinuclear zinc(II) cryptate **8** was obtained from **7** and zinc(II) in aqueous solution and was anticipated to be less reactive toward phosphates because the zinc(II) ions appeared to be coordinately saturated in a distorted trigonal-bipyramidal (five-coordinate) environment. To our surprise, **8** reacted exclusively with a phosphomonoester dianion, 4-nitrophenyl phosphate (NPP^{2-}), to produce its phosphoramidate derivative **9** (see Scheme 2), but not with bis(4-nitrophenyl) phosphate (BNP^- , a phosphodiester monoanion), tris(4-nitrophenyl) phosphate (TNP , a neutral phosphotriester), or 4-nitrophenyl acetate (NA , a neutral carboxyester), while the latter ester substrates are generally more reactive with nucleophiles derived

(5) (a) Kimura, E.; Nakamura, I.; Koike, T.; Shionoya, M.; Kodama, Y.; Ikeda, T.; Shiro, M. *J. Am. Chem. Soc.* **1994**, *116*, 4764–4771. (b) Koike, T.; Kajitani, S.; Nakamura, I.; Kimura, E.; Shiro, M. *J. Am. Chem. Soc.* **1995**, *117*, 1210–1219. (c) Kimura, E.; Kodama, Y.; Koike, T.; Shiro, M. *J. Am. Chem. Soc.* **1995**, *117*, 8304–8311.

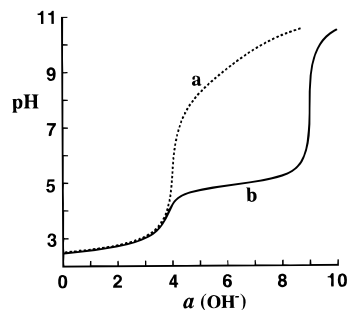


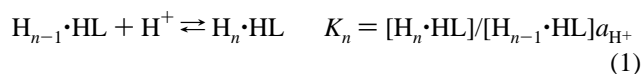
Figure 1. Typical titration curves for propanol-bridged octaazacryptand **7** at 35 °C with $I = 0.10$ (NaNO_3): (a) 1.0 mM $7 \cdot 8\text{HCl}$; (b) a + 2.0 mM $\text{Zn}^{\text{II}}\text{SO}_4$. $a(\text{OH}^-)$ is the number of equivalents of base added.

from most of the mononuclear metal complexes.^{2,4} Thus, the newly synthesized **8** was proven to be an extremely interesting cryptate to selectively recognize the phosphate dianion and cleave its P–O ester bond. Herein, we report the synthesis, structure, and reactivity of this novel cryptate **8**.

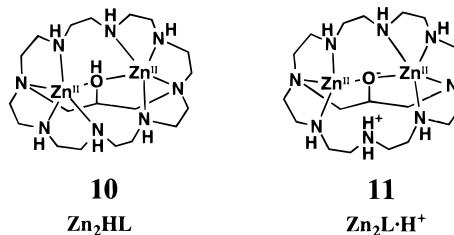
Results and Discussion

Synthesis of 26-Hydroxy-1,4,7,10,13,16,19,22-octaazabicyclo-[11.11.3]heptacosane (Propanol-Bridged Octaazacryptand 7) (Scheme 1). Contrary to our initial expectations, the reaction of [2-oxo-6-(aminomethyl)morpholy]-*N,N',N''*-triacetic acid triethyl ester (**1**) with 2 equiv of diethylenetriamine (**2**) (refluxing for 5 days) gave a new bicyclic tetraoxo intermediate **6** in 50% yield with no sign of other macrocyclic products such as **3**. Due to the rigidity of the two amido bonds, formation of the 16-membered ring in **6** is probably more facile than that of the two 12-membered rings in **3**. All the carbonyl groups were reduced with $\text{BH}_3 \cdot \text{THF}$ complex in THF to give the propanol-bridged octaazacryptand **7**, which was purified as its crystalline 8HCl salt in 33% yield.

Protonation and Zinc(II) Complexation Constants of Propanol-Bridged Octaazacryptand 7. The protonation constants (K_n) of **7** (HL) were determined by potentiometric pH titration of $7 \cdot 8\text{HCl}$ (1.0 mM) at 35 °C with $I = 0.10$ (NaNO_3). A typical pH titration curve with 1.0 mM $7 \cdot 8\text{HCl}$ is shown in Figure 1a. The titration data were analyzed for the acid–base equilibrium (eq 1), where a_{H^+} is the activity of H^+ . The mixed protonation constants $\log K_1 - \log K_8$ are 10.16 ± 0.03 , 9.27 ± 0.03 , 8.47 ± 0.02 , 7.30 ± 0.02 , 2.5 ± 0.1 , <2 , <2 , and <2 .



The titration curve of $7 \cdot 8\text{HCl}$ (1 mM) in the presence of 2 equiv of Zn^{II} (Figure 1b) reveals the formation of a stable complex at $\text{pH} > 4$, with simultaneous deprotonation of the alcohol OH, a conclusion being derived from the observation of the sole neutralization break at $a(\text{OH}^-) = 9$. Further deprotonation or precipitation of $\text{Zn}(\text{OH})_2$ was not observed at $a(\text{OH}^-) > 9$, indicating that the alkoxide-bridged zinc(II) cryptate **8** (Zn_2L) remains stable until pH ca. 12, where L is the alkoxide form of **7**. It should be noted that only the obtention of dinuclear species, **8** and its monoprotonated complex Zn_2HL **10** (or $\text{Zn}_2\text{L} \cdot \text{H}^+$ **11**) (see eqs 2 and 3), was



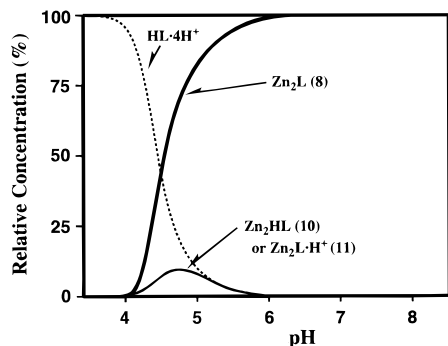
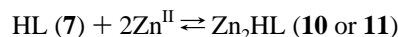
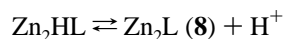


Figure 2. Distribution diagram for the zinc(II) species in 5 mM propanol-bridged octaazacryptand / 10 mM zinc(II) system as a function of pH at 35 °C.

confirmed under the experimental conditions employed. Therefore, as one zinc(II) ion binds to **7**, the second zinc(II) ion simultaneously comes in the 1:1 Zn^{II}-cryptand (e.g., ZnHL·*n*H⁺). The final structural assignment for the alkoxide O⁻-bridged dinuclear zinc(II) cryptate **8** comes from the X-ray crystal structure analysis presented below. The dinuclear zinc(II) complexation constants $K(\text{Zn}_2\text{HL})$ and deprotonation constant $K(\text{Zn}_2\text{L})$ as defined as follows:

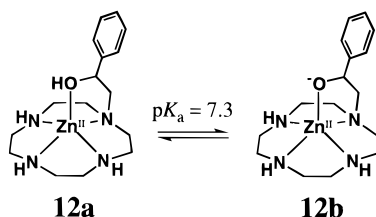


$$K(\text{Zn}_2\text{HL}) = \frac{[\text{Zn}_2\text{HL}]}{[\text{Zn}^{\text{II}}]^2[\text{HL}]} \quad (\text{M}^{-2}) \quad (2)$$



$$K(\text{Zn}_2\text{L}) = \frac{[\text{Zn}_2\text{L}]a_{\text{H}^+}}{[\text{Zn}_2\text{HL}]} \quad (\text{M}) \quad (3)$$

The obtained $\log K(\text{Zn}_2\text{HL})$ and $-\log K(\text{Zn}_2\text{L})$ values are 20.6 ± 0.1 and 4.0 ± 0.1 , respectively. A typical diagram for species distribution as a function of pH at [total zinc] = 10 mM and [total ligand] = 5 mM is displayed in Figure 2, identical conditions being used for kinetic studies described below. The extremely small $-\log K(\text{Zn}_2\text{L})$ value (i.e., deprotonation constant of **10** or **11**) indicates the facile deprotonation of the alcohol with $\text{p}K_{\text{a}} \leq 4$ involved in a double coordination with two zinc(II) ions. It is of interest to recall that the pendant alcoholic OH in 1:1 benzyl alcohol-pendant cyclen zinc(II) complex **12a** deprotonates to bind to a zinc(II) in **12b** with a larger $\text{p}K_{\text{a}}$ value of 7.3 under the same conditions.^{5c}



Previously, dinuclear zinc(II) complexation with a 24-membered monocyclic octaamine ([24]aneN₈, L') was reported by Bencini et al.⁶ In this case, a water molecule simultaneously deprotonates with a $\text{p}K_{\text{a}}$ value below 7 to bridge the two zinc(II) to yield **13** (Zn₂L'OH), which is somewhat similar to our

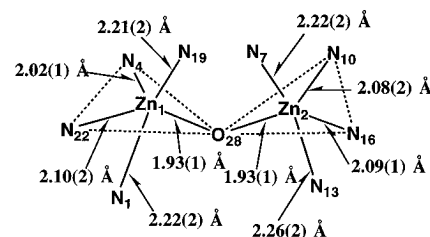
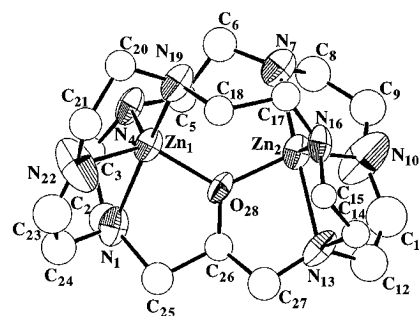
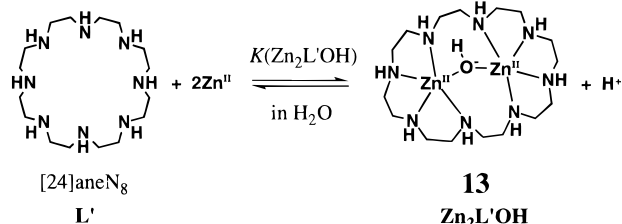
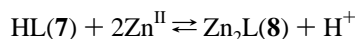


Figure 3. Crystal structure of **8** and its coordination bonding scheme with three perchlorates omitted for clarity. Thermal ellipsoids for zinc, nitrogen and oxygen atoms and circles for carbon atoms are at 30% probability level. Bond angles (deg) around zinc(II) ions are as follows: O₂₈-Zn₁-N₁, 79.2(6); O₂₈-Zn₁-N₄, 103.1(6); O₂₈-Zn₁-N₁₉, 100.7(5); O₂₈-Zn₁-N₂₂, 130.8(9); N₁-Zn₁-N₄, 84.9(7); N₁-Zn₁-N₁₉, 159.0(6); N₁-Zn₁-N₂₂, 80.2(9); N₄-Zn₁-N₁₉, 115.2(7); N₄-Zn₁-N₂₂, 118.8(9); N₁₉-Zn₁-N₂₂, 84.4(9); O₂₈-Zn₂-N₇, 102.9(6); O₂₈-Zn₂-N₁₀, 130.6(9); O₂₈-Zn₂-N₁₃, 77.7(6); O₂₈-Zn₂-N₁₆, 101.8(6); N₇-Zn₂-N₁₀, 82.5(10); N₇-Zn₂-N₁₃, 159.3(6); N₇-Zn₂-N₁₆, 115.6(7); N₁₀-Zn₂-N₁₃, 81.8(10); N₁₀-Zn₂-N₁₆, 120.2(9); N₁₃-Zn₂-N₁₆, 84.0(7).

complex. The zinc(II) complexation constant for **13**, $\log K(\text{Zn}_2\text{L}'\text{OH})$ (see eq 4), was reported to be 12.6, which is much smaller than our overall complexation constant for Zn₂L (**8**), $\log K'(\text{Zn}_2\text{L})$ of 16.6 ($= \log(K(\text{Zn}_2\text{HL})/(K(\text{Zn}_2\text{L})f_{\text{H}^+}))$, see eq 5). The comparison demonstrates the stronger stabilization by the alkoxide bridge in **8** than the external OH⁻ bridge in **13**, which is probably due to the well-preorganized ligand structure of the cryptand.

$$K(\text{Zn}_2\text{L}'\text{OH}) = \frac{[\text{Zn}_2\text{L}'\text{OH}][\text{H}^+]}{[\text{Zn}^{\text{II}}]^2[\text{L}']} \quad (\text{M}^{-1}) \quad (4)$$



$$K'(\text{Zn}_2\text{L}) = \frac{[\text{Zn}_2\text{L}][\text{H}^+]}{[\text{Zn}^{\text{II}}]^2[\text{HL}]} \quad (\text{M}^{-1}) \quad (5)$$

X-ray Crystal Structure of the Dinuclear Zinc(II) Cryptate 8. The cryptand **7** (in its acid-free form HL, see the Experimental Section) in EtOH was mixed with 2.3 equiv of Zn(ClO₄)₂ at 55 °C for 14 h. After the solvent was evaporated, the residue was crystallized from water to obtain the dinuclear zinc(II) cryptate **8**·(ClO₄)₃ as colorless crystals in 89% yield. The elemental analysis (C, H, N) suggested the formula Zn₂L·3ClO₄ containing no water. The crystal was subjected to X-ray crystal analysis. The crystal structure provided unequivocal evidence for the alkoxide-bridged dinuclear zinc(II) cryptate **8**, which is shown as an ORTEP drawing with 30% probability thermal ellipsoids for N, O, and Zn atoms and circles for C atoms in Figure 3. The methylene carbons and one of the perchlorate ions are very disordered, which is reflected upon the relatively large *R* value of 0.109. Selected crystal data and collection parameters are displayed in Table 1. Selected bond distances around zinc(II) ions are illustrated in Figure 3.

(6) Bencini, A.; Bianchi, A.; Dapporto, P.; Garcia-España, E.; Micheloni, M.; Paoletti, P. *Inorg. Chem.* **1989**, *28*, 1188–1191.

Table 1. Selected Crystallographic Data for **8**·3ClO₄ and **9**·3ClO₄·2H₂O

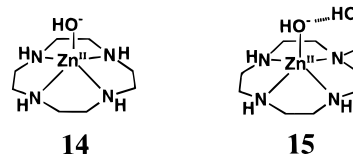
	8	9
emp form	C ₁₉ H ₄₃ N ₈ O ₁₃ Cl ₃ Zn ₂	C ₁₉ H ₄₈ N ₈ O ₁₈ Cl ₃ PZn ₂
form wt	828.7	944.7
crystal color, habit	colorless, prismatic	colorless, prismatic
crystal system	monoclinic	monoclinic
space group	<i>P</i> 2 ₁ / <i>n</i> (no. 14)	<i>Cc</i> (no. 9)
lattice params		
<i>a</i> (Å)	15.037(5)	19.573(3)
<i>b</i> (Å)	13.862(5)	12.454(4)
<i>c</i> (Å)	15.780(4)	15.066(3)
β (deg)	90.29(2)	103.94(1)
<i>V</i> (Å ³)	3289(1)	3564(1)
<i>Z</i>	4	4
<i>D</i> _{calcd} (g cm ⁻³)	1.710	1.760
μ(Cu Kα) (cm ⁻¹)	47.05	49.15
temp (°C)	20	23
scan type	ω-2θ	ω-2θ
scan rate	16.0 (9 scans)	16.0 (10 scans)
(deg min ⁻¹ , in ω)		
2θ _{max} (deg)	110.7	120.1
no. of reflns measd	total 4556	total 2896
unique 4357		unique 2778
(<i>R</i> _{int} = 0.135)		(<i>R</i> _{int} = 0.022)
structure solution	direct method	direct method
refinement	full-matrix	full-matrix
least-squares		least-squares
no. of obsns	2591	2553
(<i>I</i> > 3.00σ(<i>I</i>))		
residuals: <i>R</i> , <i>R</i> _w	0.109, 0.111	0.036, 0.051

In the cryptate **8**, both zinc(II) atoms are almost equivalent: Zn₁ (or Zn₂) is surrounded in a distorted trigonal-bipyramidal environment by the two secondary amines N₄ (or N₁₀) and N₂₂ (or N₁₆) and an alkoxide O⁻ anion (O₂₈) as equatorial donors, and the tertiary amine N₁ (or N₁₃) and another secondary amine N₁₉ (or N₇) as apical donors (see Figure 3) (later, we found that the apical NH donors N₁₉ and N₇ are labile and dissociable, see below). The average Zn-O⁻ bond distance of 1.93 Å is much shorter than that of 2.07 Å for the Zn-N equatorial bond distances and 2.23 Å for the Zn-N apical bond distances. Each zinc(II) ion lies almost in each basal plane defined by N₄, N₂₂, and alkoxide O₂₈ and N₁₀, N₁₆, and O₂₈, where the total angles around zinc(II) atoms are 352.7° (N₄-Zn₁-N₂₂, N₂₂-Zn₁-O₂₈, and O₂₈-Zn₁-N₄) and 352.6° (N₁₀-Zn₂-N₁₆, N₁₆-Zn₂-O₂₈, and O₂₈-Zn₂-N₁₀). The apical angles are bent at 159.0(6)° for N₁-Zn₁-N₁₉ and 159.3(6)° for N₁₃-Zn₂-N₇, suggesting some strain at the apical coordination sites, which is caused by the rigid ligand structure of the cryptand. The two zinc(II) ions are separated with a distance of 3.42 Å,⁷ which we later realized to be the appropriate distance to accept the two oxygen anions of phosphate.

The five-coordinate zinc(II) ions surrounded in such a rigid cryptate appeared to be coordinately almost saturated (or shielded) and, hence, initially were assumed to be totally unreactive. However, we discovered that **8** reacted with a phosphomonoester, 4-nitrophenyl phosphate (NPP²⁻), at physiological pH in aqueous solution to liberate 4-nitrophenolate.

P-O Ester Bond Cleavage of 4-Nitrophenyl Phosphate (NPP²⁻) with **8.** As an extension to our studies for intrinsic properties of zinc(II) and metallohydrolase models with macrocyclic polyamine complexes,^{4,5,8,9} we tested the reactivity of **8** with 4-nitrophenyl phosphate (NPP²⁻), bis(4-nitrophenyl) phosphate (BNP⁻), tris(4-nitrophenyl) phosphate (TNP), and 4-nitrophenyl acetate (NA). All the earlier mononuclear

complexes, Zn^{II}-cyclen **14** (cyclen = 1,4,7,10-tetraazacyclododecane)⁴ and alcohol-pendant derivatives **12b**^{5c} and **15b**^{5b}



promote hydrolysis of the neutral (TNP and NA) and monoanionic diesters (BNP⁻), but none practically reacted with the dianionic phosphomonoester NPP²⁻. This time, however, the dinuclear complex **8** selectively reacts with a phosphomonoester dianion NPP²⁻ to release 4-nitrophenol (NP) in aqueous solution (see Scheme 2). The other product was proven to be a novel intramolecularly phosphoryl oxygen-coordinating cryptate **9** (i.e., a phosphoryl-transferred complex, Zn₂L-PO₃H) by X-ray crystal analysis.¹⁰ The new complex **9** remained very stable, and we did not see any degradation of **9** (such as hydrolysis of the N-P bond) at higher pH (ca. 12) and higher temperature (ca. 60 °C) even after 1 week. Hence, we could not convert **9** back to **8** as a hydrolysis catalyst.

The ligand **7** alone at pH 8.2 (which practically exists as HL·3H⁺ on the basis of the log *K_n* values described above) and pH 6.1 (as HL·4H⁺) did not cleave the P-O ester bond at all, i.e., the same NPP²⁻ hydrolysis rates were obtained as the background reaction rates shown in dotted line of Figure 5.¹¹

Isolation of the Phosphoryl-Transferred Product (9·3ClO₄·2H₂O) and Its X-ray Crystal Structure. The phosphoryl-transferred product **9** was isolated as its triperchlorate salt in the reaction of **8** and 1.1 equiv of NPP²⁻ in aqueous solution at 60 °C for 2 days. The reaction was neat, and no other product (such as diphosphoramidate derivative) was detected by ³¹P NMR. After the solution was washed with CHCl₃ and the solvent was evaporated, the residue became crystalline from water at pH 3 in 69% yield. The elemental analysis (C, H, N) and ³¹P NMR suggested the formula **9**·3ClO₄·2H₂O. A crystal of **9**·3ClO₄·2H₂O was subjected to X-ray crystal analysis. The crystal structure is shown as an ORTEP drawing with 30% probability thermal ellipsoids in Figure 4. Selected crystal data and collection parameters are displayed in Table 1. Selected bond distances around zinc(II) ions are illustrated in Figure 4.

In the cryptate **9**, both zinc(II) ions are almost equivalent in a distorted trigonal-bipyramidal environment: Zn₁ (or Zn₂) is coordinated by the two secondary amines N₄ (N₁₀) and N₂₂ (or N₁₆) and an alkoxide O⁻ anion (O₃₁) as equatorial donors and the tertiary amine N₁ (or N₁₃) and one of the phosphoramidate anionic oxygen O₂₈ (or O₂₉) as apical donors. The average equatorial Zn-O⁻ bond distance of 2.017 Å in **9** is elongated

(8) (a) Kimura, E.; Koike, T. *Comments Inorg. Chem.* **1991**, *11*, 285–301. (b) Kimura, E. *Progress in Inorganic Chemistry*; Karlin, K. D., Ed.; John Wiley & Sons: New York, 1994; Vol. 41, pp 443–491. (c) Kimura, E.; Shionoya, M. *Transition Metals in Supramolecular Chemistry*; Fabbri, L.; Poggi, A., Eds.; Kluwer Academic Publishers: London, 1994; pp 245–259.

(9) (a) Kimura, E.; Koike, T.; Shiota, T.; Iitaka, Y. *Inorg. Chem.* **1990**, *29*, 4621–4629. (b) Kimura, E.; Koike, T.; Shionoya, M.; Shiro, M. *Chem. Lett.* **1992**, 787–790. (c) Koike, T.; Kimura, E.; Nakamura, I.; Hashimoto, Y.; Shiro, M. *J. Am. Chem. Soc.* **1992**, *114*, 7338–7345. (d) Zhang, X.; van Eldic, R.; Koike, T.; Kimura, E. *Inorg. Chem.* **1993**, *32*, 5749–5755. (e) Koike, T.; Takamura, M.; Kimura, E. *J. Am. Chem. Soc.* **1994**, *116*, 8443–8449.

(10) A similar intramolecular phosphoryl-transfer reaction with mononuclear cobalt(III) pentaammine complex and ethyl 4-nitrophenyl phosphate was reported: Hendry, P.; Sargeson, A. M. *Inorg. Chem.* **1990**, *29*, 92–97.

(11) We also synthesized a dinuclear copper(II) complex with **7** (analogous to **8**) as its triperchlorate salt, which has no activity of the NPP²⁻ ester bond cleavage under the same condition.

(7) The earlier reported dinuclear zinc(II) complex **13** was not isolated, and hence, no structural data to be compared with **8** are available.

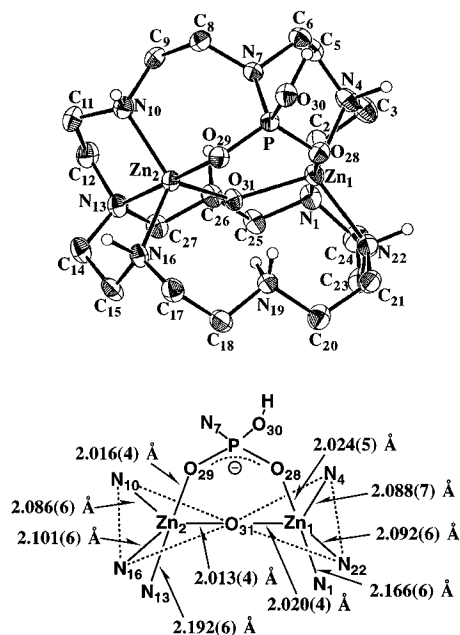


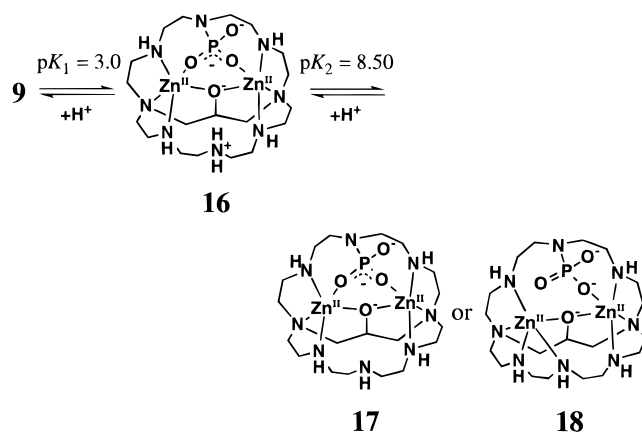
Figure 4. Crystal structure of **9** and its coordination bonding scheme with three perchlorates and two waters omitted for clarity. Thermal ellipsoids are at the 30% probability level. Bond angles (deg) around zinc(II) ions are as follows: O₂₈-Zn₁-O₃₁, 98.3(2); O₂₈-Zn₁-N₁, 178.6(2); O₂₈-Zn₁-N₄, 95.7(2); O₂₈-Zn₁-N₂₂, 97.5(2); O₃₁-Zn₁-N₁, 83.0(2); O₃₁-Zn₁-N₄, 127.0(2); O₃₁-Zn₁-N₂₂, 110.1(2); N₁-Zn₁-N₄, 83.1(2); N₁-Zn₁-N₂₂, 82.4(3); N₄-Zn₁-N₂₂, 118.3(3); O₂₉-Zn₂-O₃₁, 96.9(2); O₂₉-Zn₂-N₁₀, 95.7(2); O₂₉-Zn₂-N₁₃, 179.4(2); O₂₉-Zn₂-N₁₆, 97.6(2); O₃₁-Zn₂-N₁₀, 124.8(2); O₃₁-Zn₂-N₁₃, 83.5(2); O₃₁-Zn₂-N₁₆, 109.5(2); N₁₀-Zn₂-N₁₃, 83.6(2); N₁₀-Zn₂-N₁₆, 121.6(2); N₁₃-Zn₂-N₁₆, 82.7(2).

from 1.93 Å for **8**, along with widened Zn₁-Zn₂ distance of 3.65 Å as of 3.42 Å in **8**, which indicates the determining influence of the phosphoramidate bridging the zinc(II) ions. The apical Zn-O bond distances (2.024 and 2.016 Å) are as short as those for the equatorial Zn-O⁻ bonds (reflecting the strong Zn-O⁻(phosphoramidate) interaction). Each zinc(II) ion lies almost in each basal plane defined by N₄, N₂₂, and alkoxide O₃₁ and N₁₀, N₁₆, and O₃₁, where the total angles around zinc(II) atoms are 355.4° (N₄-Zn₁-N₂₂, N₂₂-Zn₁-O₃₁, and O₃₁-Zn₁-N₄) and 355.9° (N₁₀-Zn₂-N₁₆, N₁₆-Zn₂-O₃₁, and O₃₁-Zn₂-N₁₀). The apical angles are almost linear at 178.6(2)° for N₁-Zn₁-O₂₈ and 179.4(2)° for N₁₃-Zn₂-O₂₉, suggesting smaller strain than that shown in **8**, which is probably due to the more flexible ligand structure of the phosphoryl cryptand.

Properties of 9 and the Phosphoryl-Transfer Reaction Mechanism from 8 to 9. The cryptate **9** has two dissociable protons at the phosphoryl group and uncoordinated secondary ammonium. The deprotonation constants, pK₁ of 3.0 ± 0.1 (**9** ⇌ **16** + H⁺) and pK₂ of 8.50 ± 0.03 (**16** ⇌ **17** (or **18**) + H⁺), were found by potentiometric pH titration with **9** (1 mM) at 35 °C with *I* = 0.10 (NaNO₃). We assigned the pK₁ and pK₂ values of **9** as shown in Scheme 3. pK₁ is assigned for **9** ⇌ **16**, since it is similar to the pK_a value of 3.3 for hydrogen amidophosphate (H₂NPO₃H₂ ⇌ H₂NPO₃H⁻ + H⁺).¹² for pK₂, see the following discussion.

The reactivity of the cryptate **8** in NPP²⁻ ester bond cleavage was evaluated at various pH (9.5–4.9, 20 mM buffer) in aqueous solution at 35 °C with *I* = 0.10 (NaNO₃). The reaction (i.e., the NP production from 4-nitrophenyl phosphate) was followed by the appearance of 4-nitrophenolate at 400 nm at

Scheme 3



pH ≥ 5.9. At lower pH (5.4 and 4.9), the concentration of produced NP was determined by dilution of the test solution in 100 mM CAPS buffer (pH 10.4). The second-order dependence of the rate constant, *k*_{NPP} (M⁻¹ s⁻¹), on the concentration of **8** and on the total concentration of NPP²⁻ and its monoprotated species HNPP⁻ fits to the kinetic eq 6, where *v*_{NP} is the rate of NP production promoted by **8**. The protonation constant of NPP²⁻ (= log([HNPP⁻]/[NPP²⁻]*a*_{H⁺})) was determined to be 5.22 ± 0.03 by potentiometric pH titration at 35 °C with *I* = 0.10 (NaNO₃). The maximum *k*_{NPP} value of (1.52 ± 0.05) × 10⁻³ M⁻¹ s⁻¹ was obtained at pH 5.9.

$$v_{\text{NP}} = k_{\text{NPP}}[\mathbf{8}][\text{NPP}^{2-} + \text{HNPP}^{-}] \quad (6)$$

$$= k_{\text{obs}}[\text{NPP}^{2-} + \text{HNPP}^{-}] \quad (7)$$

The observed pseudo-first-order rate constant, *k*_{obs} (s⁻¹) for the NP production from 4-nitrophenyl phosphate (10 mM) in the presence of **8** (5 mM) is plotted as a function of pH (see Figure 5 and eq 7). The background reaction (i.e., hydrolysis of 4-nitrophenyl phosphate)¹³ in the absence of **8** was also determined using the same buffer solution (see dotted line in Figure 5). The rate vs pH profile shows a bell-shaped relationship with pK₁ of 5.2 and pK₂ of 6.3 in the acidic pH region and a pH-independent reaction with a constant *k*_{obs} value of (1.1 ± 0.1) × 10⁻⁶ s⁻¹ in the alkaline pH region (pH > 8). The kinetic pK₁ value (5.2) is almost the same as the protonation constant (*K*_a = 10^{5.22}) for NPP²⁻ + H⁺ ⇌ HNPP⁻.

We propose the overall mechanism of the P-O ester bond cleavage as shown in Scheme 4. First, the reactive form (NPP²⁻) of the phosphomonoester approaches **8** and both O⁻ donors of NPP²⁻ start to associate with suitably separated zinc(II) ions of **8** (from sixth coordination site). Simultaneously, the weakly bound apical NH's (N₇ and N₁₉) start to dissociate. Then, one of them (N₇) attacks the incoming P atom (see **19**) to release 4-nitrophenolate and form a new N-P bond. The acidic conditions (below pK₂) assist the dissociation of one of the apical NH's (N₁₉) by protonation (see **20**) so as to help the stronger association of the phosphate substrate, which accounts for the higher rate at lower pH (down to pH 5.9). We thus assign the pK₂ value of 6.3 to the protonation constant for the apical NH of the associative reaction intermediate, **19** + H⁺ ⇌ **20**. As proposed earlier (see Scheme 3), the protonated N₁₉ in the final product **9** deprotonates with a higher pK₂ (8.50) to form **17** and **18**, indicating the stronger interaction between zinc(II) and N₁₉ in the intermediate **19** than that in **9**. Further

(12) Smith, R. M.; Martell, A. E. *Critical Stability Constants*; Plenum Press: New York, 1976; Vol. 4, p 132.

(13) The pH-dependent NPP²⁻ hydrolysis at 39 °C with *I* = 1.0 was reported: Kirby, A. J.; Jencks, W. P. *J. Am. Chem. Soc.* **1965**, *87*, 3209–3216.

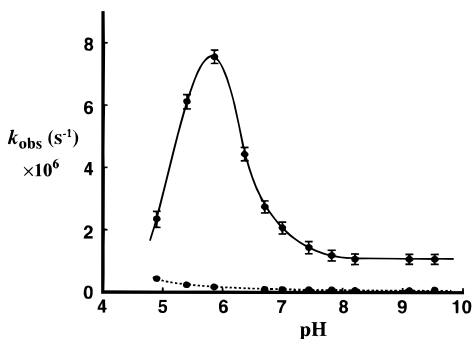
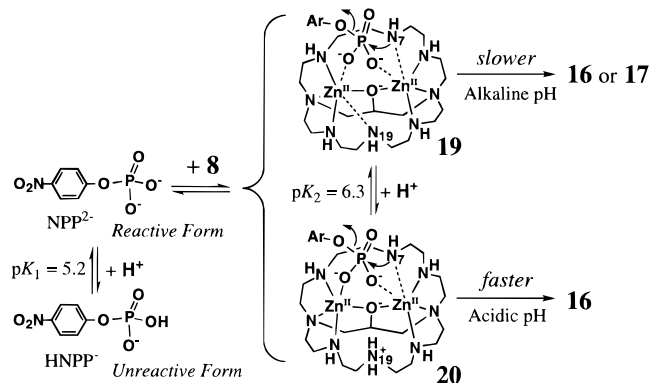
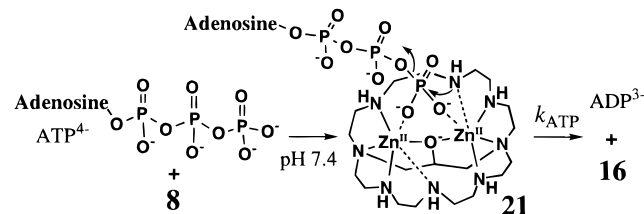


Figure 5. Rate vs pH profile for the pseudo-first-order rate constants k_{obs} (s^{-1}) of the P–O ester bond cleavage of NPP^{2-} (10 mM) in the presence of **8** (5 mM) at 35 °C. The data in a dotted line are the first-order rate constants of background reaction (NPP^{2-} hydrolysis) in the same buffer solution.

Scheme 4



Scheme 5

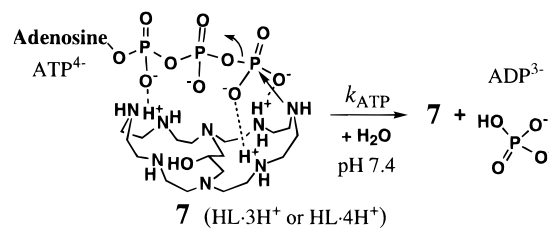


acidification, however, converts the reactive substrate NPP^{2-} into an unreactive, protonated species HNPP^- (with $\text{p}K_1$ value of 5.2), which has weaker affinity for the cryptate **8**,¹⁴ resulting in the slower reaction.

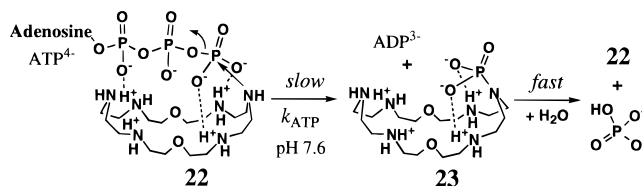
Reaction of **8 with ATP^{4-} .** In order to see if a similar phosphoryl-transfer reaction from adenosine triphosphate (ATP^{4-}) (10 mM) to **8** (10 mM) occurs, we followed the reaction by ^{31}P NMR at pH 7.4 (100 mM HEPES buffer) and 35 °C with $I = 0.5$ (NaNO_3). Indeed, the reaction took place. After 1 week, the products were identified as the phosphoryl-transferred cryptate **16** and an equimolar adenosine diphosphate (ADP^{3-}) in ca. 20% yield, along with unreacting ATP^{4-} and **8**, but no other products such as inorganic phosphate or adenosine monophosphate (AMP^{2-}) were detected. We thus propose a reaction mechanism via an ATP^{4-} -bound intermediate **21** as shown in Scheme 5, which is similar to the NPP^{2-} ester bond cleavage with **8**. The second-order rate constant k_{ATP} for our phosphoryl-transfer reaction (i.e., $\text{ATP}^{4-} + \mathbf{8} \rightarrow \text{ADP}^{3-} + \mathbf{16}$) is $(3.0 \pm 0.3) \times 10^{-5} \text{ M}^{-1} \text{ s}^{-1}$ at 35 °C.

(14) Earlier, we reported that the 1,5,9-triazacyclododecane zinc(II) complex has a larger affinity for dianionic NPP^{2-} ($K = [\text{ZnL-NPP}^{2-}]/[\text{ZnL}][\text{NPP}^{2-}] = 10^{3.1} \text{ M}^{-1}$ at 25 °C) than for monoanionic BNP^- ($K < 10^{0.5} \text{ M}^{-1}$) (see ref 4). This fact is similarly related to the smaller affinity of zinc(II) cryptate **8** for monoanionic HNPP^- .

Scheme 6



Scheme 7



As another reference experiment, the ATP^{4-} hydrolysis with the metal-free cryptand **7** (10 mM) was investigated at pH 7.4 (50 mM HEPES buffer) and 35 °C with $I = 0.5$ (NaNO_3) by ^{31}P NMR, where **7** is considered to be in the mixture of tri- and tetra-protonated forms on the basis of its $\text{p}K_a$ values. The ATP^{4-} hydrolysis was promoted by **7** with the k_{ATP} value of $(2.5 \pm 0.3) \times 10^{-5} \text{ M}^{-1} \text{ s}^{-1}$, which incidentally is almost the same as that for the phosphoryl-transfer reaction $\mathbf{8} + \text{ATP}^{4-} \rightarrow \mathbf{16} + \text{ADP}^{3-}$.¹⁵ However, unlike the reaction of the zinc(II) cryptate **8**, the products detected were inorganic phosphate and equimolar ADP^{3-} (see Scheme 6).

An analogous phosphoryl-transfer reaction was earlier reported to occur between ATP^{4-} and macrocyclic polyamines (e.g., **22**, see Scheme 7).¹⁶ The tetraprotonated macrocyclic hexaamine **22** at neutral pH is the reactive species and hydrolyzes ATP^{4-} (to ADP^{3-}) with second-order kinetics. The established mechanism involves a phosphoryl-transferred intermediate **23**, which is only transiently detected and almost immediately releases inorganic phosphate and goes back to **22**.¹⁷ One can extrapolate the second-order rate constant (k_{ATP}) of $6 \times 10^{-4} \text{ M}^{-1} \text{ s}^{-1}$ at 35 °C using the given thermodynamic activation parameters at 60 °C and pH 7.6.^{16b}

By comparing the reactions of **7** and **8** with NPP^{2-} and ATP^{4-} , it is evident that both zinc(II) ions play an additional role in stabilizing the phosphoryl-transferred species, while in the metal-free system **7**, the phosphoryl-transferred intermediate may be unstable like **23**.¹⁷ Such a function of the cooperative dinuclear zinc(II) ions may be important in phosphoryl-transfer reactions in dinuclear metallophosphatases.^{1,18}

Selective Phosphomonoester Dianion Recognition by **8** and the Relevance to Dinuclear Metallophosphatase Mechanism.

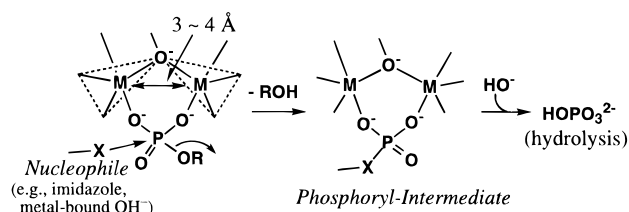
Given the finding of the selective interaction of dianionic phosphomonoester NPP^{2-} (or more anionic ATP^{4-}) with **8** in the phosphoryl-transfer mechanism and the isolation of the stable phosphoramidate bridging between each zinc(II) in **9**, we sus-

(15) Note that **7**, however, did not react with NPP^{2-} as **8** did; see above discussion.

(16) (a) Hosseini, M. W.; Lehn, J.-M.; Mertes, M. P. *Helv. Chim. Acta* **1983**, *66*, 2454–2466. (b) Hosseini, M. W.; Lehn, J.-M.; Maggiora, L.; Mertes, K. B.; Mertes, M. P. *J. Am. Chem. Soc.* **1987**, *109*, 537–544. (c) Hosseini, M. W.; Lehn, J.-M.; Jones, K. C.; Plute, K. E.; Mertes, K. B.; Mertes, M. P. *J. Am. Chem. Soc.* **1989**, *111*, 6330–6335. (d) Mertes, M. P.; Mertes, K. B. *Acc. Chem. Res.* **1990**, *23*, 413–418.

(17) Although we failed to see such an intermediate (a *N*-phosphorylated cryptand, an analogue of **23**) in our reaction of **7** with ATP^{4-} , we postulate a similar mechanism as shown in Scheme 6. The two zinc(II) ions in **9** could be removed with a 10 times excess amount of ethylenediaminetetraacetate at pH 7 and ca. 60 °C in H_2O . Then, the P–N bond of the *N*-phosphorylated cryptand was immediately hydrolyzed to yield the free cryptand **7** and inorganic phosphate, as was determined by ^1H and ^{31}P NMR.

Scheme 8



pected that inorganic phosphate dianion, HOPO_3^{2-} , might reversibly or irreversibly bind to **8** to inhibit the phosphoryl-transfer reaction $\mathbf{8} \rightarrow \mathbf{9}$. Indeed, in the presence of 10 mM HOPO_3^{2-} at pH 8.2 (20 mM TAPS) and 35 °C, the pseudo-first-order rate constant ($k_{\text{obs}} = 1.1 \times 10^{-6} \text{ s}^{-1}$) with 5 mM of **8** is reduced to $(1.9 \pm 0.1) \times 10^{-7} \text{ s}^{-1}$, supporting the notion of competitive inhibition by inorganic phosphate. However, 30 mM SCN^- , which has strong affinity to mononuclear zinc(II) (e.g., $[\text{Zn}^{\text{II}}\text{-cyclen-SCN}^-]/[\text{Zn}^{\text{II}}\text{-cyclen}][\text{SCN}^-] = 10^{2.2} \text{ M}^{-1}$ at 25 °C),^{9c} did not interfere in the reaction $\mathbf{8} \rightarrow \mathbf{9}$ under the same conditions. Accordingly, we may generalize that the selective association of phosphate dianion is feasible with the dinuclear zinc(II), provided that the distance (3–4 Å) is within a range that allows the cooperative action for the phosphate bridging and that some vacancy on the two zinc ions is available for the access of the phosphate. In this regard, the role of the strong alkoxide bridge for the simultaneous coordination to two zinc(II) should be critical (see Scheme 8). This brings both zinc(II) atoms close enough and at the same time behaves as strong equatorial donors for both zinc(II) ions. The phosphate would then access from the apical sites. In most of the dinuclear phosphatases,¹⁸ the hydroxo (HO^-), alkoxide (RO^-), or carboxylate (COO^-) ligands similarly serve as a bridging ligand between the two metal ions.

In addition, if a potential nucleophile (X in Scheme 8) is available in the vicinity, the dinuclear Zn^{II} -phosphate complex would easily be subjected to the nucleophile attack (due to the neutralization of the anionic electrophile) that leads to phosphoryl-transferred species (e.g., $\mathbf{19} \rightarrow \mathbf{16}$). An analogous phosphoryl-transfer reaction using a serine OH nucleophile and a dinuclear zinc(II) complex is well-known in phosphomonoester hydrolysis by alkaline phosphatases.¹

Recently, the X-ray crystal structure of the mammalian protein phosphatase-1 (PP-1) was reported,¹⁹ which contains two metal ions that are brought close to each other (ca. 3.3 Å) by a carboxylate oxygen anion and water (or OH^-). Each of the metal ions in PP-1 is coordinated by five ligands (such as water, imidazol, and carboxylate). The presence of two 5-coordinated metals at the active site and a histidine (or $\text{Zn}^{\text{II}}\text{-OH}^-$) nucleophile near the substrate phosphomonoester suggests structural as well as mechanistic similarities between PP-1 and **8**. In the proposed mechanism for PP-1, the substrate phosphomonoester could provide two O^- donors to the metal ions and then the ester bond cleavage reaction could proceed indirectly via a covalent phosphorylhistidine intermediate or directly with the metal-activated H_2O .

(18) (a) Karlin, K. D. *Science* **1993**, *261*, 701–708. (b) Gani, D.; Wilkie, J. *Chem. Soc. Rev.* **1995**, 55–63. (c) Purple acid phosphatase: Sträter, N.; Klabunde, T.; Tucker, P.; Witzel, H.; Krebs, B. *Science* **1995**, *268*, 1489–1492. (d) Phospholipase. C: Hough, E.; Hansen, L. K.; Birknes, B.; Jynge, K.; Hansen, S.; Hordvik, A.; Little, C.; Dodson, E.; Derewenda, Z. *Nature* **1989**, *338*, 357–360. (e) P1 nuclease: Volbeda, A.; Lahm, A.; Sakiyama, F.; Suck, D. *EMBO J.* **1991**, *10*, 1607–1618. (f) Inositol monophosphatase: Bone, R.; Frank, L.; Springer, J. P.; Atack, J. R. *Biochemistry* **1994**, *33*, 9468–9476.

(19) Goldberg, J.; Huang, H.; Kwon, Y.; Greengard, P.; Nairn, A. C.; Kuriyan, J. *Nature* **1995**, *376*, 745–753.

Conclusions

In an attempt to synthesize a bis(macrocyclic tetraamine) bridged with a 2-propyl alcohol **4**, we incidentally isolated a cryptand **7** in a good yield, which eventually gave a dinuclear zinc(II) cryptate **8** having novel functions that may be relevant to the properties of dinuclear metal-containing phosphatases. The structure of **8** was characterized by potentiometric pH-titration and X-ray crystal analysis. In the solid state, both zinc(II) ions are almost equivalent and have distorted trigonal-bipyramidal structures; an alkoxide binds both zinc(II) ions as a shared equatorial donor and two secondary amines (NH) as apical donors to each zinc(II). In aqueous solution, as a substrate phosphomonoester dianion (4-nitrophenyl phosphate) approaches in order to bridge both zinc(II) ions, the apical NH 's dissociate and one of them attacks the incoming P to perform a phosphoryl-transfer reaction (i.e., a phosphoryl group migrates from 4-nitrophenol to amine), yielding 4-nitrophenol and a new phosphoramidate-containing cryptate **16**. The product structure **9** (monoprotonated species of **16**) was fully characterized by potentiometric pH-titration and X-ray crystal analysis. The newly formed phosphoramidate bridges both zinc(II) ions in the new cryptate. The phosphoryl transfer by **8** stops at the stage of **16**, which is extremely stable, and hence **8** is not a catalyst for phosphomonoester. The zinc(II) complex **8** cleaves ATP^{4-} to yield ADP^{3-} and **16**, while the metal-free cryptand **7** (as multiprotonated species) promotes hydrolysis of ATP^{4-} to produce ADP^{3-} and inorganic phosphate. The present new findings may serve to rationalize the essence of dinuclear metallophosphatases such as selective recognition of phosphomonoesters, inhibition by inorganic phosphate, or stabilization of the phosphoryl-transferred intermediates. Suitable modification of the present serendipitous cryptand may lead to real and practical artificial phosphomonoesterase molecules.

Experimental Section

General Information. All reagents were of analytical reagent grade (purity > 99%) and were used without further purification. All aqueous solutions were prepared using distilled water. An aqueous solution of 0.10 M NaOH was made by dilution of 10 M NaOH (Merck 6495). The 10 M NaOH solution was kept in a refrigerator below 5 °C, where Na_2CO_3 is less soluble (< 1%), and taken out before raising the solution temperature. The Good's buffers (Dojindo, pK_a at 20 °C) were commercially available and were used without further purification: CAPS (3-(cyclohexylamino)propanesulfonic acid, $\text{pK}_a = 10.4$), CAPSO (3-(cyclohexylamino)-2-hydroxypropanesulfonic acid, 10.0), CHES (2-(cyclohexylamino)ethanesulfonic acid, 9.5), TAPS 3-[tris[(hydroxymethyl)methyl]amino]propanesulfonic acid, 8.4), EPPS 3-[4-(2-hydroxyethyl)-1-piperazinyl]propanesulfonic acid, 8.0), HEPES 2-[4-(2-hydroxyethyl)-1-piperazinyl]ethanesulfonic acid, 7.6), MOPS (3-morpholinopropanesulfonic acid, 7.2), and MES (2-morpholinoethanesulfonic acid, 6.2). The sodium salts of 5'-ATP· Na_2 and 5'-ADP·Na were obtained from Kohjin Co.

IR spectra were recorded on a Shimadzu FTIR-4200 spectrophotometer. ^1H (400 MHz), ^{13}C (100 MHz), and ^{31}P (162 MHz) NMR spectra at 35.0 ± 0.5 °C were recorded on a JEOL α -400 spectrometer. 3-(Trimethylsilyl)propionic-2,2,3,3- d_4 acid sodium salt in aqueous solution and tetramethylsilane in organic solution were used as internal references for ^1H and ^{13}C NMR measurements. An aqueous solution of 80% phosphoric acid was used as an external reference for ^{31}P NMR measurement. Silica gel column chromatography was carried out on Fuji Silysia Chemical FL-100D.

Synthesis of 26-Hydroxy-1,4,7,10,13,16,19,22-octaazabicyclo-[11.11.3]heptacosane Octahydrochloric Acid Salt 7·8HCl. Thionyl chloride (9.7 mL) was added dropwise to an EtOH solution (60 mL) of 2-hydroxypropylenediamine- N,N,N',N' -tetraacetic acid (10.3 g, 32 mmol) over 1 h at 0 °C. After the solution was heated to reflux for 1 day, the solvent was evaporated. The oily residue was dissolved in water (70 mL) saturated with K_2CO_3 at 0 °C, and then the solution was

extracted with CH_2Cl_2 (100 mL \times 4). After the combined organic layers were dried over anhydrous Na_2SO_4 , the solvent was evaporated. The oily residue was purified by silica gel column chromatography (eluent: $\text{CH}_2\text{Cl}_2/\text{EtOH} = 20:1$) to obtain [2-oxo-6-(aminomethyl)-morpholy]-*N,N',N'*-triacetic acid triethyl ester (**1**) as a yellowish oil (7.2 g, 58% yield). TLC (Merck Art. 5554, eluent:hexane/AcEt = 1:1): $R_f = 0.33$. IR (neat): 3463, 2984, 2940, 2909, 2874, 1740, 1449, 1416, 1372, 1345, 1194, 1098, 1069, 1030, 988, 920, 864, 733, 586 cm^{-1} . ^1H NMR (CDCl_3): δ 1.27 (6H, t, $J = 7.1$ Hz, CH_3), 1.29 (3H, t, $J = 7.1$ Hz, CH_3), 2.93 (1H, dd, $J = 7.7$ and 12.8 Hz, COOCCHN), 3.02 (1H, dd, $J = 6.7$ and 14.2 Hz, COOCCHN), 3.07 (1H, dd, $J = 5.9$ and 12.8 Hz, COOCCHN), 3.10 (1H, dd, $J = 4.9$ and 14.2 Hz, COOCCHN), 3.31 and 3.36 (2H, ABq, $J = 17.0$ Hz, NCHCO), 3.42 (1H, d, $J = 16.3$ Hz, NCHCO), 3.55 and 3.62 (4H, ABq, $J = 17.6$ Hz, NCHCO), 3.61 (1H, d, $J = 16.3$ Hz, NCHCO), 4.16 (4H, q, $J = 7.1$ Hz, OCH_2), 4.19 (2H, q, $J = 7.1$ Hz, OCH_2), 4.61 (1H, m, CCHC).

A solution of **1** (7.0 g, 18 mmol) and diethylenetriamine (**2**) (3.7 g, 36 mmol) in MeOH (400 mL) was heated to reflux for 5 days. After evaporation of the solvent, the residue was purified by silica gel column chromatography (eluent: $\text{CH}_2\text{Cl}_2/\text{MeOH}/28\% \text{NH}_3(\text{aq}) = 5:2:0.1$) followed by crystallization from CH_3CN to obtain 26-hydroxy-3,11,15,23-tetraoxo-1,4,7,10,13,16,19,22-octaazabicyclo[11.11.3]heptacosane (**6**) as colorless crystals (4.1 g, 50% yield, mp 148–149 °C). TLC (Merck Art. 5554, eluent: $\text{CH}_2\text{Cl}_2/\text{MeOH}/28\% \text{NH}_3(\text{aq}) = 5:2:0.5$): $R_f = 0.55$. IR (KBr pellet): 3463, 3296, 3088, 2940, 2830, 2368, 1649, 1551, 1485, 1472, 1465, 1443, 1343, 1269, 1167, 1130, 1100, 1055, 978, 872, 596 cm^{-1} . ^1H NMR (D_2O , pD = 5): δ 2.43 (2H, dd, $J = 10.5$ and 14.1 Hz, NCHCC), 2.66 (2H, dd, $J = 2.2$ and 14.1 Hz, NCHCC), 3.29–3.56 (12H, m, CH), 3.45 and 3.50 (8H, ABq, $J = 17.1$ Hz, NCHCO) 3.79 (1H, tt, $J = 2.2$ and 10.5 Hz, NCHCC), 3.80–3.89 (4H, m, CH). ^{13}C NMR (D_2O , pD = 5): δ 38.6, 50.9, 63.8, 64.2, 72.6, 178.3.

To a suspended solution of the tetraoxomacrocycle **6** (1.66 g, 3.6 mmol) in dry THF (33 mL) was added slowly a THF solution (75 mL) of 1 M $\text{BH}_3\cdot\text{THF}$ at 0 °C. The mixture was stirred at room temperature for 3 h and heated at 65 °C for 7 days. After decomposition of the various borane complexes with water at 0 °C, the organic solvent was evaporated. The residue was dissolved in 6 M HCl(aq) (80 mL), and the solution was heated at 70 °C for 3 h. The mixture was cooled to room temperature and washed with CH_2Cl_2 (30 mL \times 2). After the aqueous solution was concentrated to 10 mL, it was purified on an anion exchange column of Amberlite IRA-400 with water. The obtained acid-free residue was purified by silica gel column chromatography (eluent: $\text{CH}_2\text{Cl}_2/\text{MeOH}/28\% \text{NH}_3(\text{aq}) = 5:2:0.3$) followed by crystallization from 6 M HCl(aq) to obtain 26-hydroxy-1,4,7,10,13,16,19,22-octaazabicyclo[11.11.3]heptacosane, **7**·8HCl·2.5H₂O, as colorless prisms in 33% yield (269 °C dec). TLC (Merck Art. 5567, eluent: $\text{CH}_2\text{Cl}_2/\text{MeOH}/28\% \text{NH}_3(\text{aq}) = 2:2:1$): $R_f = 0.30$. IR (KBr pellet): 3440, 2988, 2780, 2689, 2484, 1617, 1574, 1472, 1375, 1329, 1074, 1005, 987, 965, 754 cm^{-1} . ^1H NMR (D_2O , pD 2): δ 2.67 (2H, dd, $J = 10.5$ and 15.6 Hz, NCHCC), 2.83 (2H, dd, $J = 1.8$ and 15.6 Hz, NCHCC), 2.98–3.12 (8H, m, NCH), 3.26–3.43 (8H, m, NCH), 3.48–3.64 (16H, m, NCH), 3.80 (1H, tt, 1.8 and 10.5 Hz, CCHC). ^{13}C NMR (D_2O , pD 2): δ 46.4, 46.8, 48.3, 55.9, 60.9, 78.1. Anal. ($\text{C}_{19}\text{H}_{57}\text{N}_8\text{O}_{3.5}\text{Cl}_8$) C, H, N: calcd, 31.0, 7.8, 15.2; found, 31.0, 7.7, 14.9.

Synthesis of Dinuclear Zinc(II) Cryptate **8·(ClO₄)₃.** The octahydrochloric acid salt **7**·8HCl·2.5H₂O (1.2 g, 1.6 mmol) was passed through an anion exchange column (Amberlite IRA-400) with water to obtain acid-free ligand **7** as a colorless oil. After dissolution of **7** in EtOH (60 mL), $\text{Zn}(\text{ClO}_4)_2\cdot 6\text{H}_2\text{O}$ (1.4 g, 3.7 mmol) was added. The solution was stirred at 55 °C for 14 h. After the solvent was evaporated, the residue was crystallized from water to obtain colorless prisms at triperchlorate salts **8**·(ClO₄)₃ in 89% yield. IR (KBr pellet): 3430, 3256, 2922, 2876, 1468, 1381, 1281, 1109, 1092, 1019, 980, 890, 845, 833, 693, 627 cm^{-1} . ^1H NMR (D_2O , pD 7): δ 2.33–3.68 (36H, m, NCH), 3.85–3.96 (1H, br, CCHC). ^{13}C NMR (D_2O , pD 7): δ 43.5, 43.9, 44.7, 45.5, 45.7, 46.0, 46.2, 46.6, 47.0, 47.4, 47.8, 47.9, 50.5, 51.0, 53.3, 53.8, 54.1, 58.9, 64.4. Anal. ($\text{C}_{19}\text{H}_{43}\text{N}_8\text{Cl}_3\text{O}_{13}\text{Zn}_2$) C, H, N: calcd, 27.5, 5.2, 13.5; found, 27.1, 5.2, 13.3.

Synthesis of Dinuclear Zinc(II) Phosphocryptate **9·(ClO₄)₃·2H₂O.** An aqueous solution (25 mL) of **8**·(ClO₄)₃ (207 mg, 0.25 mmol) and

4-nitrophenyl phosphate disodium salts (104 mg, 0.28 mmol) was stirred at 60 °C for 2 days. The solution pH was adjusted to 3 with 0.1 M HClO₄(aq). After the solution was washed with CHCl_3 (30 mL \times 5), the solvent was evaporated. The residue was crystallized from H₂O to obtain **9**·(ClO₄)₃·2H₂O as colorless prisms (163 mg, 69% yield). IR (KBr pellet): 3472, 3142, 3025, 1557, 1464, 1385, 1356, 1308, 1287, 1267, 1225, 1190, 1171, 1144, 1120, 1090, 1051, 1017, 990, 949, 918, 864, 818, 802, 691, 627 cm^{-1} . ^1H NMR (D_2O , pD 10): δ 2.44 (2H, dd, $J = 10.9$ and 12.7 Hz, CHCC), 2.55–2.74 (8H, m, NCH), 2.76 (2H, dd, $J = 2.2$ and 12.7 Hz, CHCC), 2.80–3.18 (20H, m, NCH), 3.23–3.32 (2H, m, NCH), 3.43–3.54 (2H, m, NCH), 3.87 (1H, tt, $J = 2.2$ and 10.9 Hz, CCHC). ^{13}C NMR (D_2O , pD 10): δ 45.1, 48.0, 48.1, 49.7, 51.4, 52.4, 57.1, 57.4, 60.0, 66.9. ^{31}P NMR (D_2O): 12.7 at pD 10.0, 14.2 at pD 6.3, 14.3 at pD 2.9. Anal. ($\text{C}_{19}\text{H}_{48}\text{N}_8\text{Cl}_3\text{O}_{18}\text{PZn}_2$) C, H, N: calcd, 24.2, 5.1, 11.9; found, 24.0, 5.1, 11.8.

Potentiometric pH Titrations. The pH meter (Horiba F-16) and electrode system (a pH-glass electrode and a double-junction reference electrode) was calibrated daily as follows: An aqueous solution (50.0 mL) containing 4.00 mM of HCl and 96.0 mM of NaNO₃ ($I = 0.10$) was prepared under an argon atmosphere (99.999%) at 35.0 ± 0.1 °C and then the first pH value (pH₁) was read. After 4.0 mL of 0.10 M NaOH was added to the acidic solution, the second pH value (pH₂) was read. The theoretical pH values corresponding to pH₁ and pH₂ are calculated to be pH₁' = 2.483 and pH₂' = 11.128, respectively, using $K_w (= a_{\text{H}^+}a_{\text{OH}^-}) = 10^{-13.68}$, $K_w' (= [\text{H}^+][\text{OH}^-]) = 10^{-13.48}$, and $f_{\text{H}^+} (= a_{\text{H}^+}/[\text{H}^+]) = 0.823$. The correct pH values ($-\log a_{\text{H}^+}$) can be obtained using the following equations: $a = (\text{pH}_2' - \text{pH}_1')/(\text{pH}_2 - \text{pH}_1)$; $b = \text{pH}_2' - a\text{pH}_2$; $\text{pH} = a(\text{pH-meter reading}) + b$.

The potentiometric pH titrations of **7**·8HCl (1 mM) in the presence and the absence of 2 equiv of zinc(II) were carried out at 35.0 ± 0.1 °C with $I = 0.10$ (NaNO₃) under an argon atmosphere, and two independent titrations were made. The ligand protonation constants, $K_a' = [\text{H}_n\text{L}]/[\text{H}_{n-1}\text{L}][\text{H}^+]$ (M^{-1}), deprotonation constant $K'(\text{Zn}_2\text{L}) = [\text{Zn}_2\text{L}][\text{H}^+]/[\text{Zn}_2\text{HL}]$ (M), and zinc(II) complexation constant, $K(\text{Zn}_2\text{HL}) = [\text{Zn}_2\text{HL}]/[\text{Zn}^{II}]^2[\text{HL}]$ (M^{-2}), were originally determined using a pH-titration program BEST.²⁰ All σ fit values defined in the program are smaller than 0.005. The mixed constants $K_a = [\text{H}_n\text{L}]/[\text{H}_{n-1}\text{L}][\text{H}^+]$ (M^{-1}) and $K(\text{Zn}_2\text{L}) = [\text{Zn}_2\text{L}][\text{H}^+]/[\text{Zn}_2\text{HL}]$ (M) are derived from K_a' and $K'(\text{Zn}_2\text{L})$ using $[\text{H}^+] = a_{\text{H}^+}/f_{\text{H}^+}$.

Crystallographic Study. Colorless prismatic crystals, 0.25 \times 0.20 \times 0.20 mm of **8**·(ClO₄)₃ and 0.30 \times 0.20 \times 0.10 mm of **9**·(ClO₄)₃·2H₂O, were used for data collection. The lattice parameters and intensity data were measured on a Rigaku AFC7R diffractometer with graphite monochromated Cu K α radiation and a 12-kW rotating anode generator at 20.0 and 23.0 °C, respectively. The structures were solved by direct methods (SHELXS86) and expanded using Fourier techniques (DIRDIF92). All calculations were performed using the teXsan crystal structure analysis package developed by Molecular Structure Corp. (1985 and 1992). **8**·(ClO₄)₃: Zn, N, Cl, and O atoms were refined anisotropically, while C and H atoms were refined isotropically. The final cycle of full-matrix least-squares refinement was based on 2591 observed reflections ($I > 3.00\sigma(I)$) and 337 variable parameters and converged (largest parameter was 0.09 times its esd) with $R (= \sum|F_o| - |F_c|)/\sum|F_o| = 0.109$ and $R_w (= (\sum w(|F_o| - |F_c|)^2/\sum wF_o^2)^{0.5}) = 0.111$. The carbon atoms and the oxygen atom of one of ClO₄⁻ ions are disordered at two locations. All the hydrogen atoms were not located. We attempted to determine the X-ray crystal structure of **8** at a lower temperature using liquid nitrogen, but it was unsuccessful due to the formation of cracks in the crystal. **9**·(ClO₄)₃·2H₂O: The nonhydrogen atoms were refined anisotropically, and the hydrogen atoms were included but not refined. The final cycle was based on 2553 observed reflections ($I > 3.00\sigma(I)$) and 459 variable parameters and converged (largest parameter was 0.04 times its esd) with $R = 0.036$ and $R_w = 0.051$.

Kinetic Measurements. The P–O ester bond cleavage (i.e., 4-nitrophenol and 4-nitrophenolate release reaction) rates of 4-nitrophenyl phosphate(2-) (NPP²⁻) were measured by an initial slope method (following the increase in 400-nm absorption of released 4-nitrophenolate in aqueous solution at 35.0 ± 0.5 °C. All absorbance

(20) Martell, A. E.; Motekaitis, R. J. *Determination and Use of Stability Constants*, 2nd ed.; VCH: New York, 1992.

measurements were made on a Hitachi U-3500 spectrophotometer equipped with an electric temperature controller SPR-10. Buffer (20 mM) solutions (CAPSO, pH 9.5; CHES, pH 9.1; TAPS, pH 8.2, EPPS, pH 7.8; HEPES, pH 7.4; MOPS, pH 7.0; MES, pH 6.7, 6.3, and 5.9; acetate, pH 5.4 and 4.9) were used, and the ionic strength was adjusted to 0.10 with NaNO₃. For the initial rate determination, the following typical procedure was employed: NPP²⁻ (10, 5.0, and 2.5 mM) and **8** (5.0, 2.5, and 1.0 mM) were mixed in the buffer solution, and the visible absorption increase was recorded immediately and then followed generally until ca. 0.2% formation of 4-nitrophenolate (and 4-nitrophenol), where log ϵ values for 4-nitrophenolate were 4.27 (pH 9.5), 4.26 (pH 9.1), 4.24 (pH 8.2), 4.21 (pH 7.8), 4.13 (pH 7.4), 4.00 (pH 7.0), 3.83 (pH 6.7), 3.53 (pH 6.3), and 3.08 (pH 5.9) at 400 nm. The 4-nitrophenol concentration at pH 5.4 and 4.9 was determined by dilution of the test solution in 100 mM CAPS buffer (pH 10.4), where log ϵ value for 4-nitrophenolate is 4.27. The observed first-order rate constant k_{obs} (s⁻¹) for the P–O ester bond cleavage reaction was calculated from the decay slope (4-nitrophenol and 4-nitrophenolate release rate/[NPP²⁻]). The value of $k_{\text{obs}}(1 + K_a a_{\text{H}^+})/[Zn_2L]$ gave the second-order rate constant k_{NPP} (M⁻¹ s⁻¹) for the P–O ester bond cleavage reaction. K_a is the protonation constant of NPP²⁻ (log $K_a = \log([\text{HNPP}^-]/[\text{NPP}^{2-}]a_{\text{H}^+}) = 5.22 \pm 0.03$ at 35 °C with $I = 0.10$ (NaNO₃), where HNPP⁻ is the monoprotonated species of NPP²⁻. The products (i.e., phosphoramidate derivative **9** and 4-nitrophenol) were identified by ³¹P and ¹H NMR. The control reaction for NPP²⁻ hydrolysis in the absence of **8** was performed with the same buffer solutions. Na₂HPO₄ and NaSCN were used for anion inhibition study.

The terminal P–O–P bond cleavage (i.e., the phosphoryl-transfer reaction **8** → **9**) rates of ATP⁴⁻ (10 mM) with **8** (10 mM) were determined in pH 7.4 HEPES buffer (100 mM) with $I = 0.5$ (NaNO₃) by the time-dependent change in the integrals from the resolved ³¹P NMR signals of ATP⁴⁻, ADP³⁻, inorganic phosphate, and phosphor-

amide derivative **9**. The NMR measurement was carried out until ca. 20% P–O–P bond cleavage by the non-decoupling method at 35.0 ± 0.5 °C. The calculated standard deviation for the observed second-order rates was within 10%. The control reactions for ATP hydrolysis in the absence of **8** were performed with the same buffer solution. The ATP (10 mM) hydrolysis reaction with ligand **7** (10 mM) was determined under the same conditions apart from buffer (50 mM HEPES, pH 7.4).

Kinetics procedures for reaction of **8** (5.0 and 10 mM) with 4-nitrophenyl acetate,^{5b} bis(4-nitrophenyl) phosphate,^{5c} and tris(4-nitrophenyl) phosphate⁴ are the same as previously reported with macrocyclic polyamine zinc(II) complexes.

Acknowledgment. We are thankful to the Ministry of Education, Science and Culture in Japan for financial support by a Grant-in-Aid for Scientific Research (B) (No. 07458144) for E.K. and by a Grant-in-Aid for Scientific Research (C) (No. 07807206) for T.K. T.K. thanks the Ciba-Geigy Foundation (Japan) for the Promotion of Science for financial support. An NMR instrument in the Research Center for Molecular Medicine (RCMM) of Hiroshima University was used.

Supporting Information Available: Tables of crystallographic parameters, atomic coordinates, equivalent isotropic temperature factors, anisotropic temperature factors, bond lengths, and bond angles in CIF format for **8**·(ClO₄)₃ and **9**·(ClO₄)₃·2H₂O. Ordering information is given on any current masthead page.

JA953413M